Thermodynamic Properties of Holographic Multiquark and the Multiquark Star

P. Burikham[1,2*], E. Hirunsirisawat[1†], S. Pinkanjanarod[1,3‡]

[1] *Theoretical High-Energy Physics and Cosmology Group, Department of Physics, Faculty of Science, Chulalongkorn University, Bangkok 10330, Thailand*

[2] *Thailand Center of Excellence in Physics, Ministry of Education, Bangkok, Thailand*

[3] *Department of Physics, Faculty of Science, Kasetsart University, Bangkok 10900, Thailand*

June 14, 2010

Abstract

We study thermodynamic properties of the multiquark nuclear matter. The dependence of the equation of state on the colour charges is explored both analytically and numerically in the limits where the baryon density is small and large at fixed temperature between the gluon deconfinement and chiral symmetry restoration. The gravitational stability of the hypothetical multiquark stars are discussed using the Tolman-Oppenheimer-Volkoff equation. Since the equations of state of the multiquarks can be well approximated by different power laws for small and large density, the content of the multiquark stars has the core and crust structure. We found that most of the mass of the star comes from the crust region where the density is relatively small. The mass limit of the multiquark star is determined as well as its relation to the star radius. For typical energy density scale of 10 GeV/fm^3, the converging mass and radius of the hypothetical multiquark star in the limit of large central density are approximately $2.6-3.9$ solar mass and 15-27 km. The adiabatic index and sound speed distributions of the multiquark matter in the star are also calculated and discussed. The sound speed never exceeds the speed of light and the multiquark matters are thus compressible even at high density and pressure.

*Email:piyabut@gmail.com, piyabut.b@chula.ac.th

†Email:ekapong.hirun@gmail.com, ekapong.h@student.chula.ac.th

‡Email:quazact@gmail.com, Sitthichai.P@student.chula.ac.th

1 Introduction

All of the high energy experiments which fail to produce a free quark are strong evidences that the coupling constant of the strong interaction becomes nonperturbatively large at low energy and large distance. Quarks and gluons are said to be confined within hadrons and the colourless condition becomes a requirement of an assembly of quarks at low energy. However, when the energy or temperature scale of a system of quarks and gluons increases, the coupling of the strong interaction tends to be weaker and finally we expect the deconfinement to occur. In addition, if the quarks and gluons are compressed extremely tightly together, quarks could interact with neighbouring quarks and gluons equally and become effectively deconfined from the mesonic or baryonic bound state. In the latter case, the coupling could still be strong despite of the deconfinement. Nevertheless, we could also have the situation where gluons are deconfined but the quarks are not completely free due to the remaining Coulomb-type potential from gluon exchanges between quarks.

Recently, the experimental results from collision of heavy ions suggested that the nuclear deconfinement phase might have been created in the laboratory and we might have produced the quark-gluon plasma (QGP). The RHIC experiment revealed that the produced QGP behaves like fluid with very small viscosity. However, this property of small viscosity fluid is hard to be understood in the picture of QGP as the gas of free quarks and gluons. Additionally, lattice simulations show that QGP has relatively high pressure right above the deconfinement temperature T_c which is again difficult to explain using the weakly coupled quarks and gluons gas [1, 2, 3]. It is possible that various coloured and colour-singlet bound states of quarks and gluons could exist in the plasma at the temperature $(1-3)T_c$ [4, 3, 5]. The existence of the coloured bound states could explain the problems of high pressure, small viscosity, and the jet quenching of the QGP at once.

Due to the large coupling of the strong interaction at low energies, a perturbative method has limited applicability to the high energy processes and phenomena. The development of the holographic principle and AdS/CFT correspondence [6] provides us with a new method to investigate the physics of strongly coupled nuclear matter both in the low energy regime and in the energy scale close to the deconfinement temperature. Holographic models of meson were proposed by Juan Maldacena, Soo-Jong Rey, Stefan Theisen, Jung-Tay Yee [7, 8, 9]. The Coulomb potential plus screening effect of quark and antiquark are calculated from the Nambu-Goto action of the string in the bulk spacetime at zero and finite temperature. For baryons, Witten, Gross and Ooguri [10, 11] proposed a holographic baryon to be a D-brane wrapping internal subspace of the background spacetime with N_c strings connected and stretching out to the boundary. For $AdS_5 \times S^5$, the baryon vertex is a D5-brane wrapping the S^5. The basic requirement is that a total of N_c charges from the endpoint of the strings cancel with the charge of the vertex itself. A generalization of this condition allows more strings to go in and come out of the vertex, as long as the total charges from all of the string endpoints add up to N_c [12, 13, 14, 15, 16, 17]. Baryon vertex plus strings configuration in this case represent the holographic multiquark states. Generically they have colour charges but because of the confinement, they can only exist in the deconfined phase.

The coloured multiquark phase can be studied in the general Sakai-Sugimoto model (SS)[18,

19] in the intermediate temperature above the gluon deconfinement but below the chiral symmetry restoration temperature [20]. It was found that the multiquark phase is thermodynamically stable and preferred over the other phases in the gluon-deconfined plasma provided that the density is sufficiently large [17]. The situation of high density and moderate temperature could exist inside certain classes of compact stars and it is thus interesting to investigate the thermodynamical properties of the multiquark nuclear matter as well as their contributions to the stability of the dense stars. In this article, we will consider the hypothetical multiquark star which obeys the equation of state derived from the holographic multiquarks in the SS model. With the power-law approximation of the equations of state, we study its gravitational stability using the Tolman-Oppenheimer-Volkoff equation (TOV)[21]. The mass, density and pressure distributions are obtained numerically. The mass-radius relation and the mass limit are also discussed. Corresponding hydrodynamical properties such as the sound speed of the multiquark nuclear matter are explored within the star. The multiquark matters are found to be compressible throughout the entire multiquark star.

This article is organized as the following. Section 2 describes the holographic setup for the multiquarks and the multiquark phase in the gluon-deconfined SS model. The thermodynamic relations and the equations of state of the multiquark nuclear matter are calculated and discussed in Section 3 and 4. In Section 5, the Einstein field equation for the spherically symmetric star is solved to obtain the TOV equation. Assuming the equations of state derived in Section 3 and 4 for the multiquark nuclear matter, we explore the gravitational physics of a hypothetical multiquark star. A mass-radius relation is derived and some discussion on the more realistic situation is commented. The adiabatic index and the sound speed of the multiquark nuclear matter within the star are studied. Section 6 concludes the article.

2 Holographic multiquark configuration

Since string theories in the bulk spacetime correspond to certain gauge theories on the boundary of that space, it is natural to find construction of the bound states of quarks in the form of strings and branes. While the meson is proposed to be the string hanging in the bulk with both ends locating at the boundary of the AdS space [7], the baryon is proposed to be the Dp-brane wrapped on the S^p with N_c strings attached and extending to the boundary of the bulk space [10, 11].

On the gauge theory side, hadrons exist in the confined phase as a result of the linear part of the binding potential. However, the bound states of quarks can actually exist in the deconfined phase at the intermediate temperatures above the deconfinement as well. Even though gluons are free to propagate and the linear potential is absent, the quarks can form bound state through the remaining Coulomb-type potential due to the colour charges of the quarks.

The holographic model of non-singlet bound state was also proposed. As is demonstrated in Ref. [17], we can modify the Witten's baryon vertex by attaching more strings to the vertex provided that the total number of charges of all of the strings are preserved to N_c. Some

strings may extend along radial direction of the AdS space down to the horizon and some can extend to the boundary. We define the number of strings that extend to the boundary to be k_h and the number of strings extending radially to the horizon to be k_r. The restriction of k_h and k_r is due to the force condition of the string configuration (see Ref. [17] for details).

In this article, we consider the holographic model of multiquarks in the Sakai-Sugimoto (SS) model [18, 19] similar to the configurations considered in Ref. [17]. The background metric of the bulk spacetime in the SS model in a deconfined phase at finite temperature is given by

$$ds^2 = \left(\frac{u}{R_{D4}}\right)^{3/2}\left(f(u)dt^2 + \delta_{ij}dx^i dx^j + dx_4{}^2\right) + \left(\frac{R_{D4}}{u}\right)^{3/2}\left(u^2 d\Omega_4^2 + \frac{du^2}{f(u)}\right).$$

The four-form field strength, the dilaton, and the curvature radius of the spacetime are

$$F_{(4)} = \frac{2\pi N}{V_4}\epsilon_4, \qquad e^{\phi} = g_s\left(\frac{u}{R_{D4}}\right)^{3/4}, \qquad R_{D4}^3 \equiv \pi g_s N l_s^3,$$

respectively, where $f(u) \equiv 1 - u_T^3/u^3$, $u_T = 16\pi^2 R_{\rm D4}^3 T^2/9$. x_4 is the compactified coordinate transverse to the probe D8/$\overline{\rm D8}$ branes with arbitrary periodicity $2\pi R$. The volume of the unit four-sphere Ω_4 is denoted by V_4 and the corresponding volume 4-form by ϵ_4. $F_{(4)}$ is the 4-form field strength, l_s is the string length and g_s is the string coupling.

In the SS model, the chiral symmetry dynamics is taken into account, by construction, in the form of the dynamics of the flavour branes, D8 and $\overline{\rm D8}$. The DBI action of D8-$\overline{\rm D8}$ is

$$S_{D8} \;=\; -\mu_8 \int d^9X e^{-\phi} Tr\sqrt{-det(g_{MN} + 2\pi\alpha' F_{MN})} \tag{1}$$

where F_{MN} is the field strength of the flavour group $U(N_f)$ on the branes. It is given by

$$F = d\mathcal{A} + i\mathcal{A}\wedge\mathcal{A}. \tag{2}$$

The $U(N_f)$ gauge field $\mathcal{A}$ can be decomposed into $SU(N_f)$ part A and $U(1)$ part $\hat{A}$:

$$\mathcal{A} = A + \frac{1}{\sqrt{2N_f}}\hat{A}, \tag{3}$$

where only the diagonal $U(1)$ will be turned on here. Lastly, g_{MN} is the induced metric on the D8-branes world volume.

In the deconfined phase, the equation of motion from the action of D8-$\overline{\rm D8}$ provides 3 possible configurations: (i) connected D8-$\overline{\rm D8}$ without sources in the bulk representing the vacuum state and (ii) the parallel configuration of both D8-branes and $\overline{\rm D8}$ representing the χ_S-QGP. Another stable configuration (iii) is the connected D8-$\overline{\rm D8}$ branes with the D4-brane as the baryon vertex submerged and localized in the middle of the D8 and $\overline{\rm D8}$.[1] In

[1] Actually, the quark matter, represented by the connected D8-$\overline{\rm D8}$ branes with radial strings stretching out to the horizon, is another possible configuration satisfying the equation of motion. However, it was found that this phase is thermodynamically unstable to density fluctuations by Bergman, Lifschytz, and Lippert [22].

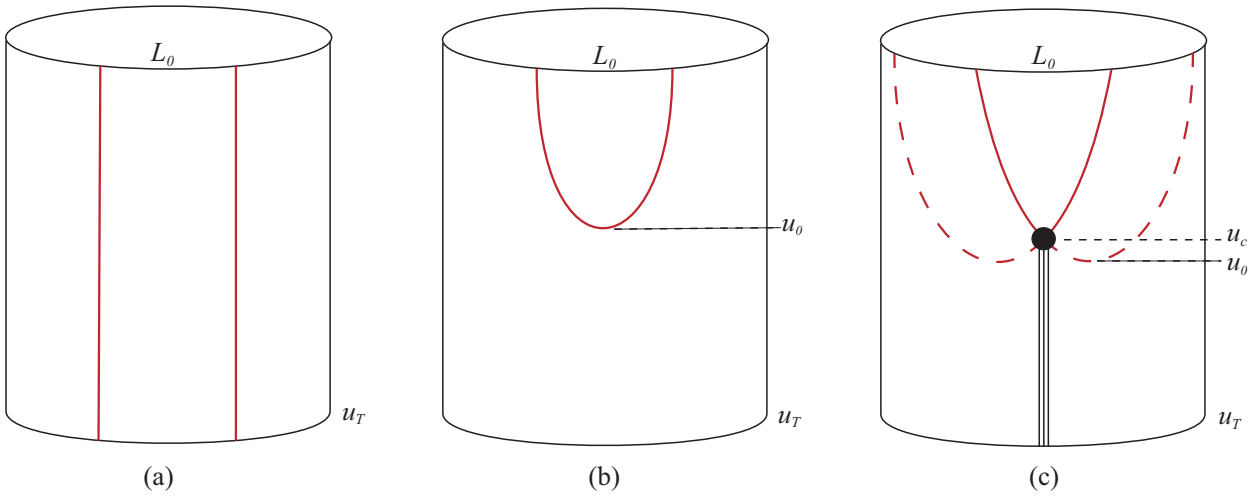

Figure 1: Different configurations of D8 and $\overline{\text{D8}}$-branes in the background field following the Sakai-Sugimoto model that are dual to the phases of (a) χ_S-QGP, (b) vacuum and (c) multiquark phase.

this model, we assume that the hanging strings shrink to approximately zero and the only apparent strings are the k_r radial strings. The three configurations are shown in Fig. 1. We will consider the thermodynamic properties of only the last multiquark configuration. The action of the exotic multiquark phase is given by

$$S = S_{D8} + S_{D4} + \tilde{S}_{F1}, \tag{4}$$

where S_{D8} is the DBI action of the connected D8-branes, S_{D4} represents the DBI action of the D4-brane wrapped on S^4 and $\tilde{S}_{F1}$ is the action of k_r radial strings extending from the baryon vertex down to the horizon. For simplicity, we ignore the distortion of the baryon vertex due to the Chern-Simon term [23, 24].

The DBI action of the D8-$\overline{\text{D8}}$-brane coupled to the diagonal U(1) gauge field is given by

$$S_{D8} = \mathcal{N}\int_{u_c}^{\infty} du\, u^4\sqrt{f(u)(x_4'(u))^2 + u^{-3}(1-(\hat{a}_0'(u))^2)}, \tag{5}$$

where the constant $\mathcal{N} = (\mu_8\tau N_f\Omega_4 V_3 R^5)/g_s$, and the rescaled $U(1)$ diagonal field $\hat{a} = 2\pi\alpha'\hat{A}/(R\sqrt{2N_f})$. Position of the vertex is denoted by u_c, it is determined from the equilibrium condition of the D8-D4-strings configuration (see Appendix A of Ref. [17]). The source action of the D4 and strings, $S_{D4} + \tilde{S}_{F1}$, are given by

$$S_{source} = \mathcal{N}d\left[\frac{1}{3}u_c\sqrt{f(u_c)} + n_s(u_c - u_T)\right], \tag{6}$$

where n_s is the number of radial strings k_r in the unit of N_c. The number of radial strings n_s represents the colour charges of a multiquark. For a fixed number of k_h, one of the radial

strings can merge with another radial string from another multiquark and form a colour-binding potential between the two in a similar way holographic meson is formed between a quark and an antiquark.

The $U_B(1)$ symmetry corresponds to the $U(1)$-diagonal part of the global flavor symmetry, $U(N_f)$, which is provided by the N_f flavor branes. Naturally, the baryon chemical potential, conjugating to the $U_B(1)$ charge, in the gauge theory side can be identified with the boundary value of the zero component of the gauge field in the flavor branes, i.e. A_0, conjugating to the $U(1)$ "electric" charge. For convenience, our normalized baryon chemical potential is [25]

$$\mu = \hat{a}_0(\infty). \tag{7}$$

In gauge-gravity duality, we identify the grand canonical potential density in the gauge theory side in the form of the D8-branes action evaluated with the classical solution [26]:

$$\Omega(\mu) \;=\; \frac{1}{\mathcal{N}} S_{D8}[T, x_4'(u), \hat{a}_0(u)]_{cl} \tag{8}$$

With the additional source term, the free energy is in the form of the combination of the Legendre-transform of the grand potential and the source action, Eqn. (6). The baryon chemical potential is simply the derivative of the free energy with respect to its conjugate, i.e. the baryon number density, at a particular temperature:

$$\mu = \frac{\partial}{\partial d}\frac{1}{\mathcal{N}}\left(\tilde{S}_{\rm D8}[T, x_4'(u), d(u)]_{cl} + S_{\rm source}(d, u_c)\right) \tag{9}$$

where the Legendre-transformed action $\tilde{S}_{\rm D8}$ is given by

$$\tilde{S}_{\rm D8}[T, x_4'(u), d(u)] \;=\; S_{D8}[T, x_4'(u), \hat{a}_0(u)] + \mathcal{N}\int_{u_c}^{\infty} d(u)\hat{a}_0' du \tag{10}$$

$$\;=\; \int_{u_c}^{\infty} du u^4 \sqrt{f(u)(x_4'(u))^2 + u^{-3}}\sqrt{1 + \frac{d(u)^2}{u^5}}, \tag{11}$$

where $d(u)$ is the electric displacement. It is a constant of the configuration given by

$$d(u) = -\frac{1}{\mathcal{N}}\frac{\delta S_{D8}}{\delta \hat{a}_0'(u)} = \frac{u\hat{a}_0'(u)}{\sqrt{f(u)(x_4'(u))^2 + u^{-3}(1 - (\hat{a}_0'(u))^2)}} = \text{const.} \tag{12}$$

Note that the Legendre transformation changes the dependence on the variable $\hat{a}_0(u)$ in S_{D8} to $d(u)$ in $\tilde{S}_{D8}$. As a result, the grand potential as a function of the baryon chemical potential is transformed into the free energy as a function of the baryon number density. Another constant of the configuration is

$$(x_4'(u))^2 \;=\; \frac{1}{u^3 f(u)}\Big[\frac{f(u)(u^8 + u^3 d^2)}{F^2} - 1\Big]^{-1} = \text{const.}, \tag{13}$$

where F is a function of u_c, d, T and n_s, given by

$$F^2 = u_c^3 f_c\left(u_c^5 + d^2 - \frac{d^2\eta_c^2}{9f_c}\right), \tag{14}$$

where $\eta_c \equiv 1 + \frac{1}{2}\left(\frac{u_T}{u_c}\right)^3 + 3n_s\sqrt{f_c}$. For convenience, here and henceforth, f, f_c and f_0 are used to represent $f(u)$, $f(u_c)$ and $f(u_0)$, respectively. Note that this form of F is derived from the force condition at the cusp u_c. The detailed calculations are given in the Appendix of Ref. [17].

With the equation of motion for x_4, Eqn. (13), and the separation between D8- and $\overline{\text{D8}}$-branes L_0 being fixed to $L_0 = 2\int_{uc}^{\infty} x_4'(u)du = 1$, we obtain [22]

$$\mu = \int_{u_c}^{\infty} \hat{a}_0'(u) + \frac{1}{\mathcal{N}} \frac{\partial S_{source}}{\partial d}\bigg|_{T,L_0,u_c}, \tag{15}$$

where the second term is the contribution from the sources, μ_{source}. From these relations, we can then study the thermodynamic properties of the multiquark phase. The phase diagram of the multiquark nuclear phase is studied in Ref. [17] when the colour-binding interaction is neglected. It is found that multiquarks are preferred thermodynamically over the other gluon-deconfined phases for the large density and intermediate temperature below the chiral symmetry restoration temperature.

3 Calculations of the equation of state

Thermodynamic properties of the nuclear/exotic matter phase can be described by the equation of state. First, we will investigate the relations between the pressure and the number density. From the previous section (see also Ref. [17]), the grand potential density and the chemical potential of the nuclear/exotic matters are given by

$$\Omega = \int_{u_c}^{\infty} du \left[1 - \frac{F^2}{f(u)(u^8 + u^3 d^2)}\right]^{-1/2} \frac{u^5}{\sqrt{u^5 + d^2}}, \tag{16}$$

$$\mu = \int_{u_c}^{\infty} du \left[1 - \frac{F^2}{f(u)(u^8 + u^3 d^2)}\right]^{-1/2} \frac{d}{\sqrt{u^5 + d^2}} + \frac{1}{3} u_c \sqrt{f(u_c)} + n_s(u_c - u_T) \tag{17}$$

respectively.

Since the differential of the grand potential G_Ω can be written as

$$dG_\Omega = -PdV - SdT - Nd\mu \tag{18}$$

where the state parameters describing the system P, V, S, T, N are the pressure, volume, entropy, temperature, the total number of particles of the system respectively. Since the change of volume is not our concern, we define the volume density of G_Ω, S and N to be Ω, s and d, respectively. Therefore, we have, at a particular T and μ,

$$P = -G_\Omega/V \equiv -\Omega(T, \mu). \tag{19}$$

By assuming that the multi-quark states are spatially uniform, we obtain

$$d = \frac{\partial P}{\partial \mu}(T, \mu). \tag{20}$$

Using the chain rule,

$$\left.\frac{\partial P}{\partial d}\right|_T = \left.\frac{\partial \mu}{\partial d}\right|_T d, \tag{21}$$

so that

$$P(d,T,n_s) = \mu(d,T,n_s)\ d - \int_0^d \mu(d',T,n_s)\ \mathrm{d}(d'), \tag{22}$$

where we have assumed that the regulated pressure is zero when there is no nuclear matter, i.e. $d = 0$.

In the limit of very small d, u_c approaches u_0, η_c becomes $\eta_0 + \mathcal{O}(d)$, where η_0 is defined to be η_c with u_c replaced by u_0. From Eqn. (17), the baryon chemical potential can then be approximated to be

$$\mu - \mu_{source} \simeq d\left\{ \int_{u_c}^{\infty} du \left[1 - \frac{u_0^8 f_0}{f u^8} - \frac{f_0 u_0^3 \left(1 - \frac{\eta_0^2}{9f_0} - \frac{u_0^5}{u^5}\right) d^2}{f u^8}\right]^{-1/2} u^{-5/2}\left(1 - \frac{d^2}{2u^5}\right)\right\}, \tag{23}$$

where $\mu_{source} = \frac{1}{3} u_c \sqrt{f(u_c)} + n_s(u_c - u_T)$, and we have neglected the higher order terms of d. By using the binomial expansion, the above equation becomes

$$\begin{aligned} \mu - \mu_{source} &\simeq d\left\{ \int_{u_0}^{\infty} du \frac{u^{-5/2}}{\sqrt{1 - \frac{f_0 u_0^8}{f u^8}}} \left[1 + \left(\frac{f_0 u_0^3}{f u^8 - f_0 u_0^8}\left(1 - \frac{\eta_0^2}{9f_0} - \frac{u_0^5}{u^5}\right) - \frac{1}{u^5}\right)\frac{d^2}{2}\right]\right\} \\ &= \alpha_0 d - \beta_0(n_s) d^3, \end{aligned} \tag{24}$$

where

$$\alpha_0 \equiv \int_{u_0}^{\infty} du \frac{u^{-5/2}}{1 - \frac{f_0 u_0^8}{f u^8}}\ , \tag{25}$$

$$\beta_0(n_s) \equiv \int_{u_0}^{\infty} du \frac{u^{-5/2}}{2\sqrt{1 - \frac{f_0 u_0^8}{f u^8}}} \left(\frac{f_0 u_0^3}{f u^8 - f_0 u_0^8}\left(1 - \frac{\eta_0^2}{9f_0} - \frac{u_0^5}{u^5}\right) + \frac{1}{u^5}\right). \tag{26}$$

By substituting Eqn.(24) into Eqn.(22), we can determine the pressure in the limit of very small d as

$$P \simeq \frac{\alpha_0}{2} d^2 - \frac{3\beta_0(n_s)}{4} d^4. \tag{27}$$

In the limit of very large d and relatively small T,

$$\mu - \mu_{source} = \int_{u_c}^{\infty} du \left[1 - \frac{f_c u_c^3}{f u^3}\left(\frac{u_c^5 + d^2 - \frac{d^2 \eta_c^2}{9 f_c}}{u^5 + d^2}\right)\right]^{-1/2} \frac{d}{\sqrt{u^5 + d^2}} \tag{28}$$

$$\approx \int_{u_c}^{\infty} du \frac{d}{\sqrt{u^5 + d^2}} + \frac{1}{2} u_c^3 f_c d^2 \left(1 - \frac{\eta_c^2}{9 f_c}\right) \int_{u_c}^{\infty} du \frac{d}{f u^3 (u^5 + d^2)^{3/2}} \tag{29}$$

$$\approx \frac{d^{2/5}}{5} \frac{\Gamma\left(\frac{1}{5}\right)\Gamma\left(\frac{3}{10}\right)}{\Gamma\left(\frac{1}{2}\right)} + \frac{u_c^3 f_c}{10}\left(1 - \frac{\eta_c^2}{9 f_c}\right) d^{-4/5} \frac{\Gamma\left(-\frac{2}{5}\right)\Gamma\left(\frac{19}{10}\right)}{\Gamma\left(\frac{3}{2}\right)} \tag{30}$$

where we have used the fact that the lower limit of integration u_c^5/d^2 is approximately zero as d is very large. Again by using Eqn.(22), we obtain

$$P \simeq \frac{2}{35}\left(\frac{\Gamma\left(\frac{1}{5}\right)\Gamma\left(\frac{3}{10}\right)}{\Gamma\left(\frac{1}{2}\right)}\right) d^{7/5}. \tag{31}$$

And the energy density can then be found via the relation $d\rho = \mu d(d)$.

Next we consider the entropy of the multiquarks phase. From the differential of the free energy,

$$dF_E = -PdV - SdT + \mu dN, \tag{32}$$

the entropy is given by

$$S = -\frac{\partial F_E}{\partial T}. \tag{33}$$

The entropy density can then be written as

$$s = -\frac{\partial \mathcal{F}_E}{\partial T}, \tag{34}$$

where $\mathcal{F}_E$ is the free energy density which relates to the grand potential density as $\mathcal{F}_E = \Omega + \mu d$. Since we have the pressure $P = -\Omega$, we can write

$$s = \frac{\partial P}{\partial T} - \left(\frac{\partial \mu}{\partial T}\right) d. \tag{35}$$

For both small d and large d, we can see from the formula of the pressure (see Eqn.(27),(31), noting that α_0, β_0 is insensitive to temperature) and the chemical potential (see Eqn.(24),(30)), that the dominant contribution comes only from μ_{source}, thus

$$s \simeq -\left(\frac{\partial \mu_{source}}{\partial T}\right) d. \tag{36}$$

The baryon chemical potential from the D8-branes is insensitive to the changes of temperature. This implies that the main contribution to the entropy density of the multiquark nuclear phase comes from the source term namely the vertex and strings.

Since

$$\frac{\partial \mu_{source}}{\partial T} = \frac{\partial}{\partial T}\left(\frac{1}{3}u_c\sqrt{f(u_c)} + n_s(u_c - u_T)\right), \tag{37}$$

$$\frac{\partial \mu_{source}}{\partial T} \approx -\frac{\left(\frac{16\pi^2}{9}\right)^3 T^5}{u_0^2\sqrt{1-\left(\frac{u_T}{u_0}\right)^3}} - n_s\frac{32\pi^2 T}{9}, \tag{38}$$

where we have used the fact that u_c is approximately constant with respect to the temperature in the range between the gluon deconfinement and the chiral symmetry restoration (see

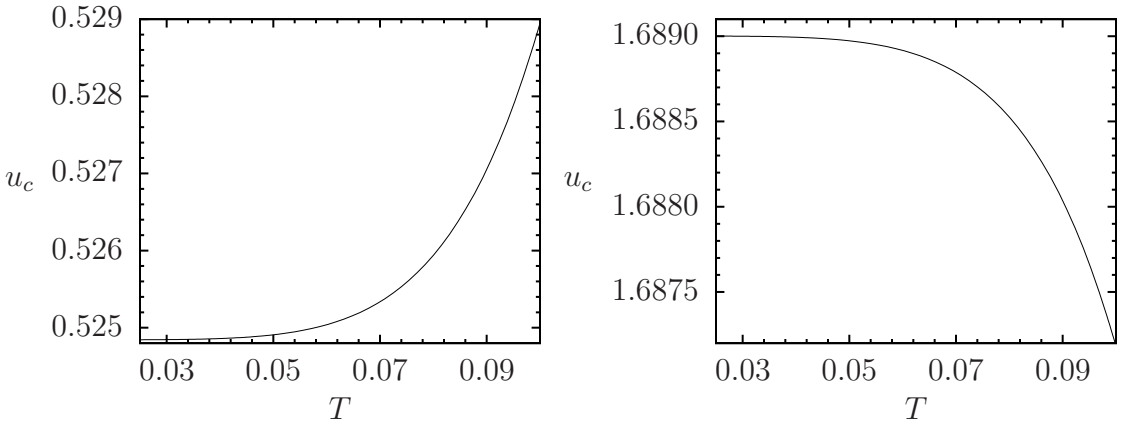

Figure 2: The graphs show the relations between u_c and T at small density (left) and at large density (right).

Fig. 2). Therefore, we obtain

$$s \approx \frac{\left(\frac{16\pi^2}{9}\right)^3 T^5 d}{u_0^2\sqrt{1-\left(\frac{u_T}{u_0}\right)^3}} + n_s\frac{32\pi^2 T d}{9}. \tag{39}$$

For small n_s, the entropy density is proportional to T^5. When n_s gets larger (carrying colour charge), the entropy density becomes dominated by the colour term $s \propto n_s T$. This is confirmed numerically in Section 4. It has been found that the entropy density of the χ_S-QGP scales as T^6 [22] corresponding to the fluid of mostly free quarks and gluons. We can see that the effect of the colour charge of the multiquarks as quasi-particles is to make them less like free particles with the temperature dependence $\sim n_s T$, i.e. much less sensitive to the temperature.

It is interesting to compare the dependence of pressure on the number density, Eqn. (27) and (31), to the confined case at zero temperature studied in Ref. [28]. The power-law relations for both small and large density of the confined and deconfined multiquark phases are in the same form (for $n_s = 0$). The reason is that the main contributions to the pressure for both phases are given by the D8-branes parts and they have similar dependence on the density for both phases. For the deconfined multiquark phase, the additional contributions from the source terms in Eqn. (17), μ_{source}, are mostly constant with respect to the density (this is because u_c becomes approximately independent of d for small and large d limits).

Consequently, when we substitute into Eqn. (22), the constant contributions cancel out and affect nothing on the pressure.

On the contrary, the entropy density for the deconfined phase is dominated by the contributions from the sources namely the vertex and strings. The contribution of the D8-branes is insensitive to the change of temperature and therefore does not affect the entropy density significantly. The additional source terms, however, depend on the temperature and thus contribute dominantly to the entropy density. Once the temperature rises beyond the gluon-deconfined temperature, entropy density will rise abruptly (for sufficiently large density d) and become sensitive to the temperature according to Eqn. (39), due to the release of quarks from colourless confinement appearing as the sources. However, we will see later on using the numerical study in Section 4 that for low densities and for small n_s, the numerical value of the entropy density is yet relatively small.

4 Numerical studies of the thermodynamic relations

From the analytic approximations in the previous section, we expect the pressure to appear as straight line in the logarithmic scale for small and large d with the slope approximately 2 and 7/5 respectively. The relation between pressure and density of the multiquarks from the full expressions can be plotted numerically as are shown in Fig. 3-5. The pressure does not really depend much on the temperature and we therefore present only the plots at $T = 0.03$. Remarkably, the transition from small to large d is clearly visible in the logarithmic-scale plots. The transition occurs around $d_c \simeq 0.072$. Interestingly, as is shown in Fig. 5, the multiquarks with larger n_s has lower pressure than the ones with smaller n_s for $d < d_c$ and *vice versa*. The dependence on n_s remains to be seen for small d as we can see from Eqn. (27). For large d, the n_s-dependence is highly suppressed as predicted by Eqn. (31).

The entropy density as a function of the temperature for various ranges of the density is shown in Fig. 6. The temperature dependence for both small and large d are the same, $\simeq T^5$ at the leading order. The d-dependence is linear and thus appears as separation of straight lines in the logarithmic-scale plot. For $n_s > 0$, we can see from Eqn. (39) that the linear term in T should become increasingly important. This is confirmed numerically as is shown in Fig. 6. The slope of the graph between the entropy density s and T in the double-log scale for $n_s = 0$ (the left plot) and $n_s = 0.3$ (the right plot) is approximately 5 and 1 respectively. Regardless of the temperature dependence, it should be noted that the numerical value of the entropy density for small densities and low n_s in Fig. 6 is quite small.

Lastly, the relations between the baryon number density and chemical potential are shown in Fig. 7. Temperature has very small effect on these curves and negligible for the range of temperature between the gluon deconfinement and the chiral-symmetry restoration. The baryon chemical potential depends linearly on the number density for small d. For large d, the relation between the chemical potential and number density becomes $\mu \approx d^{2/5}$. Interestingly, the multiquark quasi-particles behave more like fermions as a result of being the electric response of the DBI action [22].

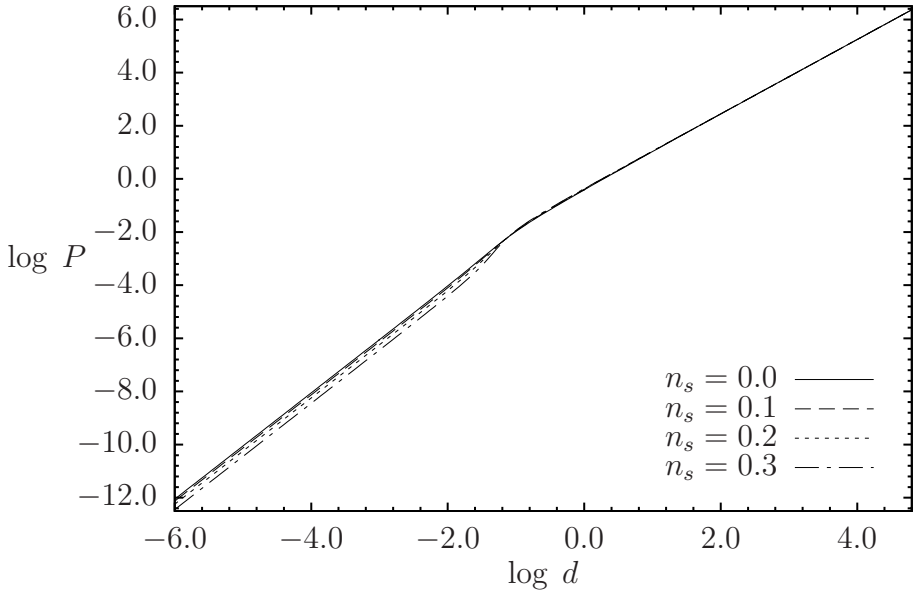

Figure 3: Pressure and density in logarithmic scale at $T = 0.03$.

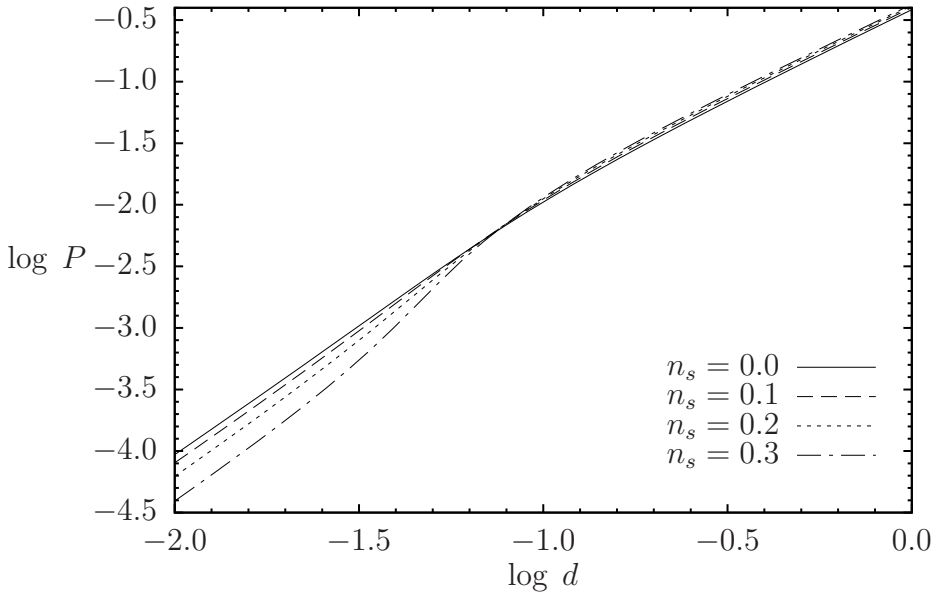

Figure 4: Pressure and density in logarithmic scale at $T = 0.03$, zoomed in around the transition region.

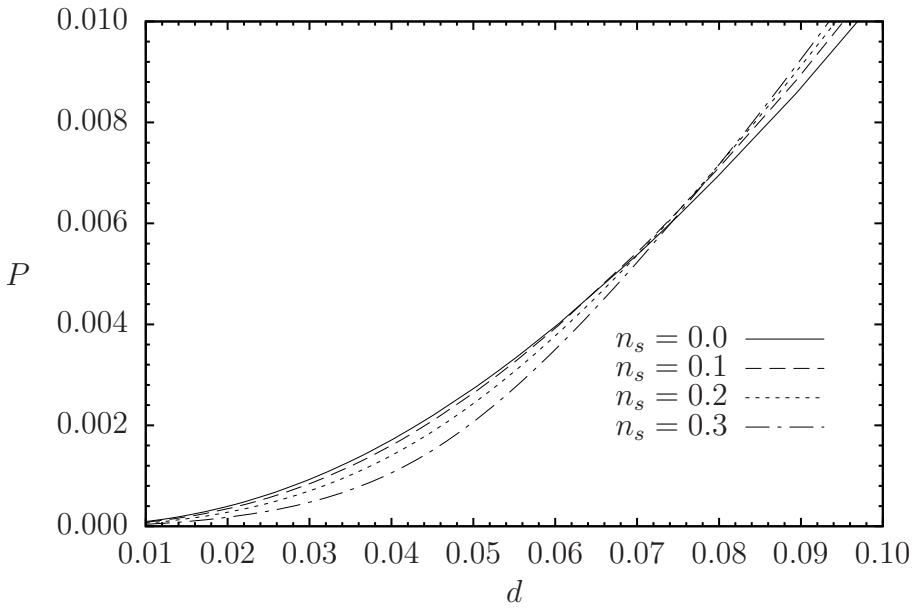

Figure 5: Pressure and density in linear scale.

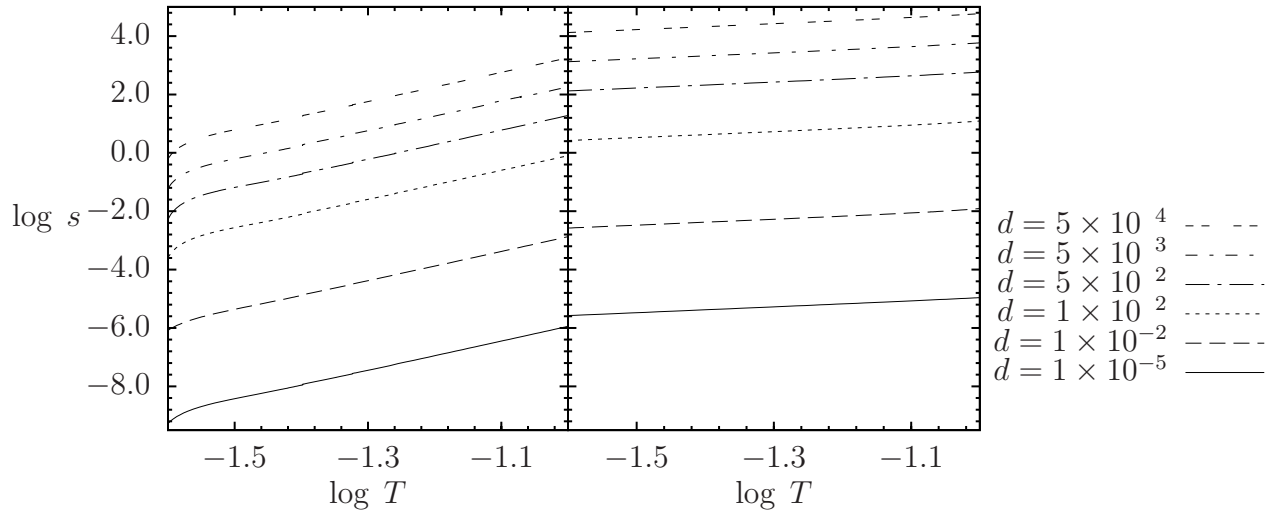

Figure 6: Entropy and temperature in logarithmic scale for $n_s = 0$ (left), 0.3 (right).

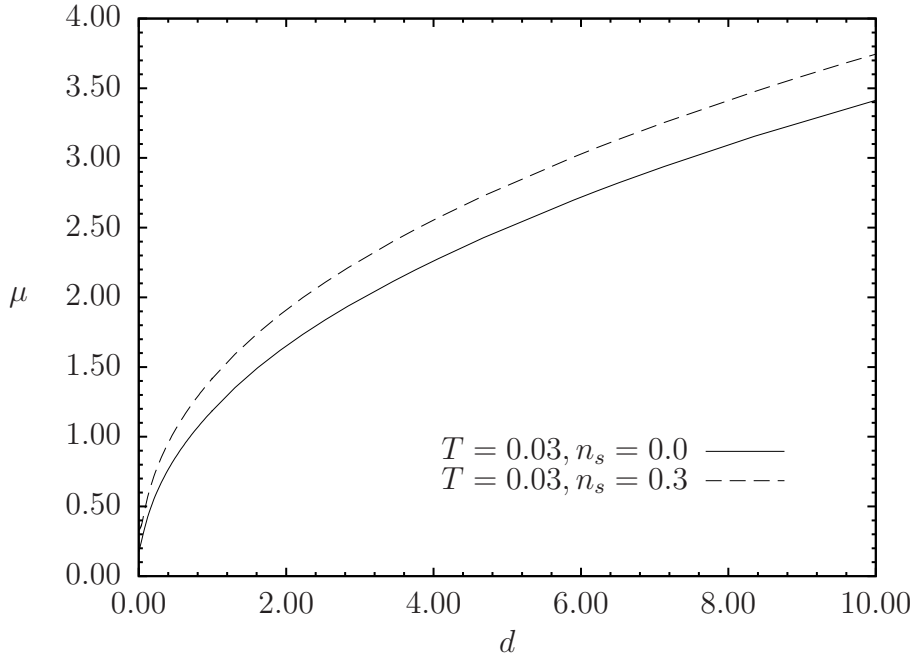

Figure 7: The baryon chemical potential and number density in logarithmic scale at $T = 0.03$.

5 Gravitational stability of the dense multiquark star

When a dying star collapses under its own gravity, it is generically believed that the degeneracy pressure of either electrons or neutrons would be able to stop the collapse to form a white dwarf or a neutron star. If the star is more massive than the upper mass limit of the neutron star, it would collapse into a black hole eventually. The mass limit of the neutron star is sensitive to the physics of warm dense nuclear matter but little is known about the equation of state of nuclear matter under high temperature and large density. Even though the original mass limit of the neutron star estimated by Oppenheimer, and Volkoff was only 0.7 solar mass [21], the new limit when the nuclear interactions are included could be as large as 2.5 solar mass [27]. Under extreme pressure and density, the quarks within hadrons could be freed and wander around the interior of the star. In other words, quarks are effectively deconfined from the localized hadrons but confined by gravity within the star. Using the bag model to describe the state of being confined by gravity but possibly deconfined from the hadrons, it turns out that quark matter phase, e.g. strange star, is possible under extreme pressure and density.

However, physics of the deconfinement is largely unknown due to the non-perturbative nature of the strong interaction and the difficulty of lattice approach to deal with finite baryon density situation. The bag model are not always served as a reliable theoretical tool to explore the behaviour of quarks in the dense star when the deconfinement exists. It is therefore interesting to use the equation of state of the deconfined nuclear matter from the holographic model to investigate the behaviour of the dense star as a complementary tool

to the bag model and other approaches.

In this section, we will consider a hypothetical multiquark star containing only the multiquark matter with uniform constant temperature. The relations between pressure and density will be adopted directly from the holographic model as the equations of state of the quasi-particles. Since the pressure and density have very small temperature dependence for the range of temperatures under consideration, the results are valid generically.

A study into the gravitational stability of a spherically symmetric dense star can be performed using the Tolman-Oppenheimer-Volkoff equation [21]. It is known that the spherically symmetric dense star has metric in a form

$$ds^2 = A(r)dt^2 - B(r)dr^2 - r^2 d\Omega_2. \tag{40}$$

After substituting into the Einstein field equation, we obtain the following relations,

$$B(r) = \left(1 - \frac{A^*(r)}{r}\right)^{-1}, \tag{41}$$

$$\frac{dA^*(r)}{dr} = 8\pi\rho r^2, \tag{42}$$

and

$$\frac{dP(r)}{dr} = -\frac{(\rho + P)}{2}\frac{A'(r)}{A(r)} = -\frac{(\rho + P)}{2}\frac{8\pi P r^3 + A^*(r)}{r(r - A^*(r))}. \tag{43}$$

The last equation is known as the Tolman-Oppenheimer-Volkoff (TOV) equation. The accumulated mass of the star, $M(r)$, is given by $A^*(r) = 2M(r)$. It has been shown in Ref. [29] that the chemical potential can be defined through the background metric in the form of $\mu(r) = \frac{\epsilon_F}{\sqrt{A(r)}}$. It will automatically solve the TOV equation. Note that the constant ϵ_F is arbitrary. Since

$$\frac{\mu'(r)}{\mu(r)} = -\frac{1}{2}\frac{A'(r)}{A(r)}, \tag{44}$$

the TOV equation becomes

$$\frac{dP(r)}{dr} = (\rho + P)\frac{\mu'(r)}{\mu(r)}. \tag{45}$$

Together with the first law of thermodynamics $\rho + P = \mu d$, the TOV equation then takes the following form,

$$d\mu = \frac{1}{d}\left(\frac{\partial P}{\partial d}\right) d(d). \tag{46}$$

Obviously, the chemical potential can be determined, as a function of the number density:

$$\mu(d) = \int_0^d \frac{1}{\eta}\left(\frac{\partial P}{\partial \eta}\right) d\eta + \mu_{onset}, \tag{47}$$

where $\mu_{onset} \equiv \mu(d = 0)$. Additionally, considering from the TOV equation together with the first law of thermodynamics, the density $d\rho = \mu d(d)$ can be integrated to

$$\rho(d) = \int_0^d \left[\int_0^\eta \frac{1}{\eta'}\left(\frac{\partial P}{\partial \eta'}\right) d\eta' + \mu_{onset}\right] d\eta. \tag{48}$$

For a power-law equation of state, $P = kd^\lambda$, the chemical potential, Eqn. (47), becomes

$$\mu(d) = \frac{\lambda k}{\lambda - 1} d^{\lambda - 1} + \mu_{onset}, \tag{49}$$

and eventually the equation of state is given by

$$\rho = \frac{1}{\lambda - 1} P + \mu_{onset} \left(\frac{P}{k} \right)^{1/\lambda}. \tag{50}$$

In our holographic model of multiquarks, the relation between pressure and density has a unique power-law behaviour, as is also found in Ref. [22] for the case of normal baryon ($n_s = 0$). This is shown in Fig. 3-4. For small d, $P \propto d^2$ ($n_s = 0$) and for large d, $P \propto d^{7/5}$. The dependence on n_s becomes significant when the density d is small and the equation of state can be approximated by $P \simeq \alpha d^2 + \beta d^4$. Since there are two power-laws governing, we need to match the solutions from the two regions together (i.e. *core* and *crust*). The number density where the equation of state changes from the large-d to the small-d is denoted by d_c.

For $n_s = 0$, at the transition point $d = d_c$, the energy density is given by Eqn. (50),

$$\rho_c = \frac{k' d_c^{\lambda'}}{\lambda' - 1} + \mu_{onset} d_c, \tag{51}$$

where $P = k' d^{\lambda'}$ (Eqn. (27) suggests that $\lambda' = 2$) is the equation of state of the small d region. We recalculate the relation Eqn. (47), (48) for the large d region which match with this ρ_c to be

$$\mu = \mu_c + \lambda k \left(\frac{d^{\lambda - 1}}{\lambda - 1} - \frac{d_c^{\lambda - 1}}{\lambda - 1} \right), \tag{52}$$

$$\rho = \rho_c + \frac{1}{\lambda - 1} P + \mu_c \left[\left(\frac{P}{k} \right)^{1/\lambda} - d_c \right] + k d_c^\lambda - \frac{\lambda k}{\lambda - 1} d_c^{\lambda - 1} \left(\frac{P}{k} \right)^{1/\lambda}. \tag{53}$$

Numerical results and Eqn. (31) suggest that $\lambda = 7/5$ for the large d region.

For $n_s > 0$, assume the equation of state for small d is in the form of $P = ad^{\lambda_1} + bd^{\lambda_2}$ (Eqn. (27) suggests that $\lambda_{1,2} = 2, 4$), the chemical potential and energy density for the small d region become

$$\mu = \mu_{onset} + \frac{\lambda_1 a d^{\lambda_1 - 1}}{\lambda_1 - 1} + \frac{\lambda_2 b d^{\lambda_2 - 1}}{\lambda_2 - 1}, \tag{54}$$

$$\rho = \mu_{onset} d + \frac{a d^{\lambda_1}}{\lambda_1 - 1} + \frac{b d^{\lambda_2}}{\lambda_2 - 1}. \tag{55}$$

We obtain the transition density in the similar fashion,

$$\rho_c = \mu_{onset} d_c + \frac{a d_c^{\lambda_1}}{\lambda_1 - 1} + \frac{b d_c^{\lambda_2}}{\lambda_2 - 1}. \tag{56}$$

Numerical results show that for large d, the effect of n_s is negligible. Therefore, the baryon chemical potential and the density for the large d region are again given by Eqn. (52) and (53). The equations of state, Eqn. (50),(53) as well as the corresponding relations for $n_s > 0$ case, are in the mixed form containing both the quasi-particle nonlinear terms and the linear term. The linear term is roughly $\rho_{linear} \approx 2.5P$ and the quasi-particle term is approximately $\rho_{quasi} \approx P^{5/7}$.

We can solve the TOV equation when the equations of state are given as above by starting from the core of the star out to the surface. As we go from the center towards the surface of the star, the density decreases until it reaches a critical value ρ_c. This density corresponds to the number density d_c where the power-law changes from $P \simeq d^{7/5}$ to $P \simeq d^2$ (see Fig. 3-4). For the crust region where the density $\rho < \rho_c$, multiquarks obey a different equation of state given by Eqn. (50). The radius of the core is defined to be the distance R_{core} where $\rho(R_{core}) = \rho_c$ and the surface of the star is defined to be the radial distance R where $\rho(R) = 0$.

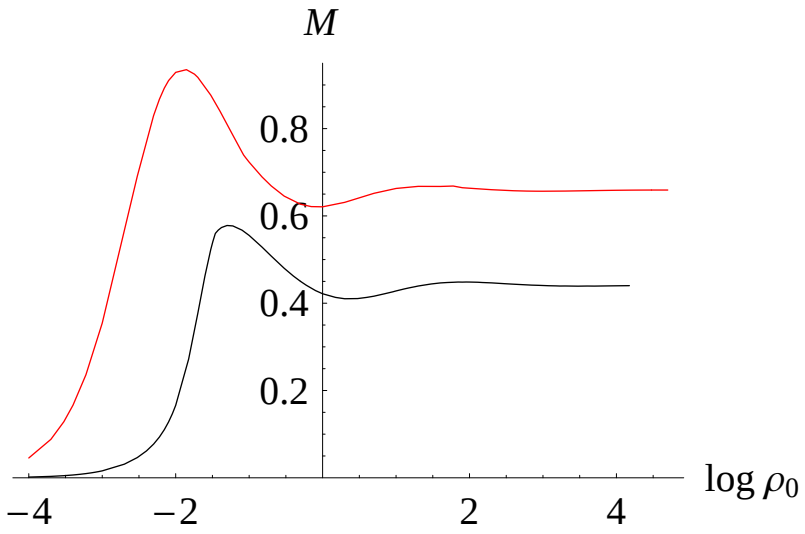

Figure 8: The relation between mass and central density of the multiquark star for multiquarks with $n_s = 0$ (upper), 0.3 (lower).

For $n_s = 0$, numerical fittings suggest that $k = 10^{-0.4}, \lambda = 7/5, d_c = 0.215443, \mu_c = 0.564374$ (core) and $k' = 1, \lambda' = 2, \mu_{onset} = 0.17495$ (crust). For $n_s = 0.3$, good fit parameters are $k = 10^{-0.4}, \lambda = 7/5, d_c = 0.086666, \mu_c = 0.490069$ (core) and $a, b = 0.375, 180.0, ; \lambda_{1,2} = 2, 4; \mu_{onset} = 0.32767$ (crust). Varying the central density ρ_0 of the star, we obtain the mass-density relation in Fig. 8. Each curve has two maxima, a larger one in the small density region and a smaller one in the large density region. Each maximum corresponds to each power-law of the equation of state, the low density to the crust and the large density to the core. Interestingly, the contribution to the total mass of the multiquark star comes dominantly from the crust. This is shown in Fig. 9. Even though the density is much lower, the volume of the crust is proportional to the second power of the radius and thus makes the contribution of the crust to the total mass larger than the core's.

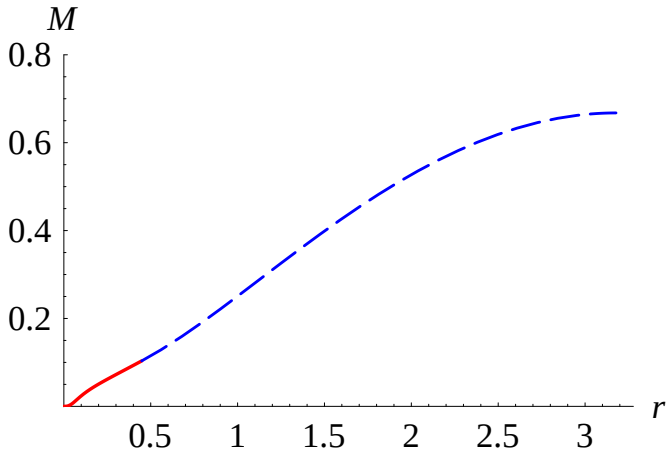

Figure 9: The accumulated mass distribution in the hypothetical multiquark star for the central density $\rho_0 = 20$ and $n_s = 0$. The inner (outer) red (dashed-blue) line represents the core (crust) region.

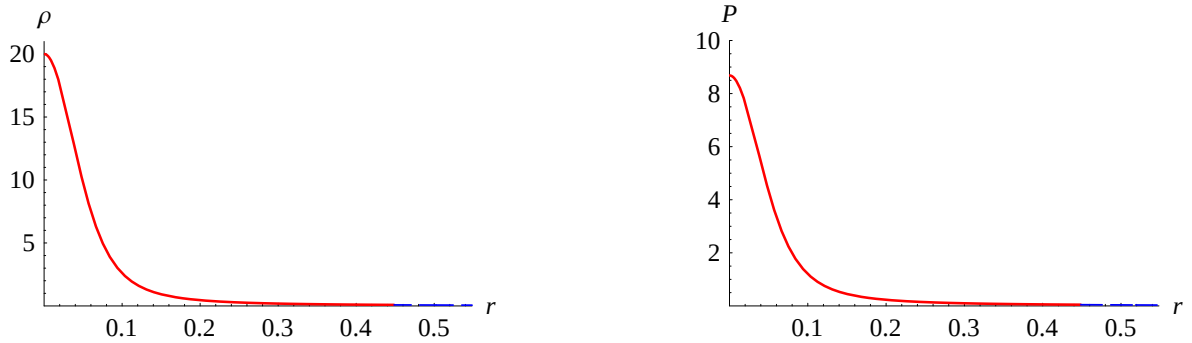

Figure 10: The density, and pressure distribution in the hypothetical multiquark star for the central density $\rho_0 = 20$ and $n_s = 0$. The inner (outer) red (dashed-blue) line represents the core (crust) region.

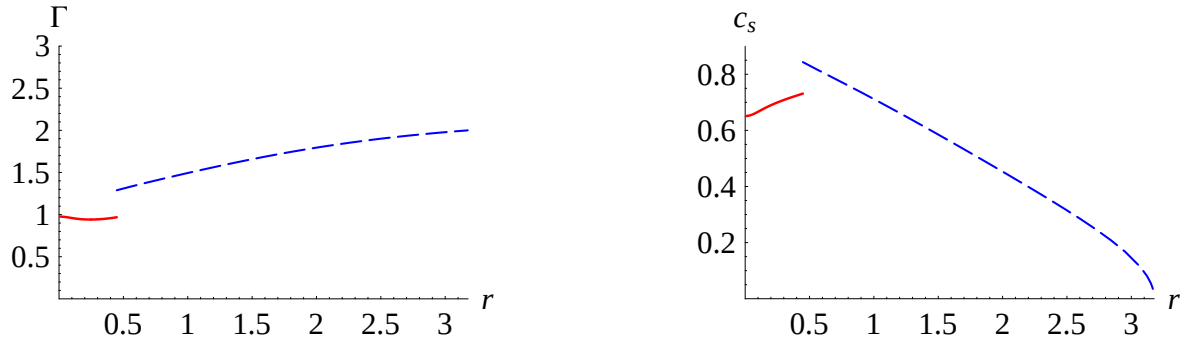

Figure 11: The adiabatic index at constant entropy (Γ) and the sound speed (c_s) distribution in the hypothetical multiquark star for the central density $\rho_0 = 20$ and $n_s = 0$. The inner (outer) red (dashed-blue) line represents the core (crust) region.

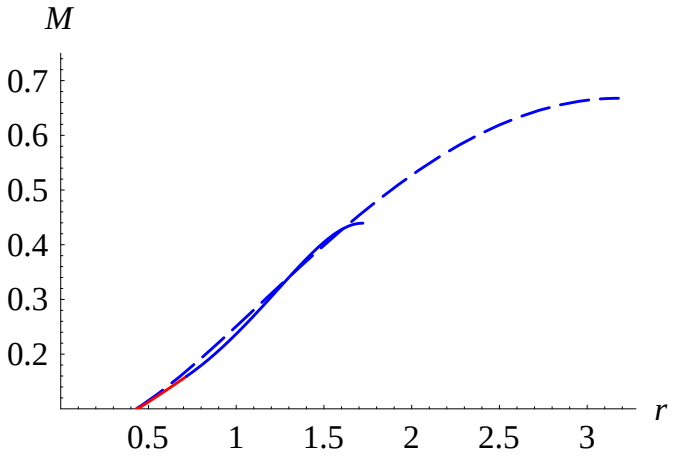

Figure 12: Comparison of the accumulated mass distribution in the hypothetical multiquark star for the central density $\rho_0 = 20$ between $n_s = 0$ and 0.3. The (dashed) blue line represents the crust region of multiquark star with $n_s = 0.3$ (0). The red lines represent the core region of which both cases are almost the same.

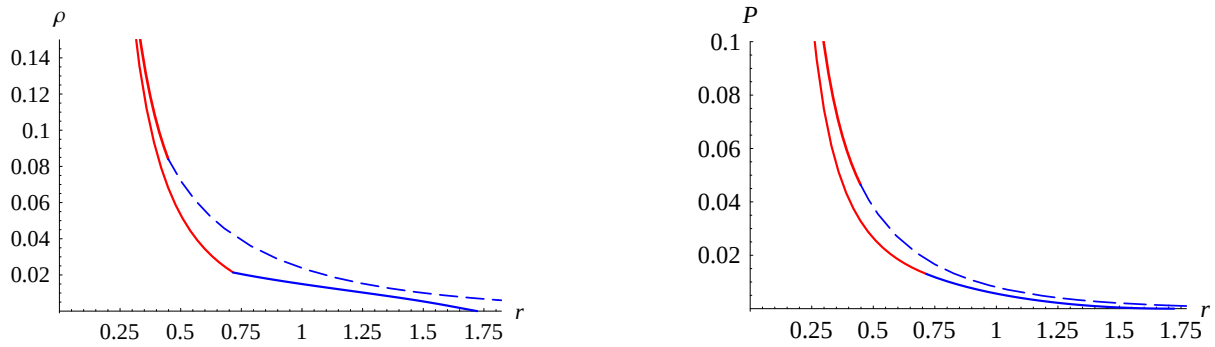

Figure 13: Comparison of the density, and pressure distribution in the hypothetical multiquark star for the central density $\rho_0 = 20$ between $n_s = 0$ and 0.3. The (dashed) blue line represents the crust region of multiquark star with $n_s = 0.3$ (0). The red lines represent the core region of which both cases are almost the same.

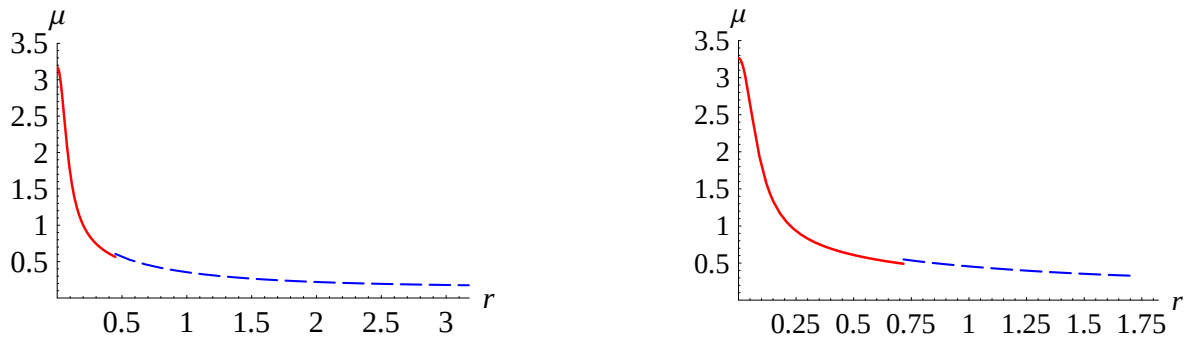

Figure 14: Comparison of the baryon chemical distributions in the hypothetical multiquark star for the central density $\rho_0 = 20$ between $n_s = 0$ (left) and 0.3 (right). The solid (dashed) red (blue) line represents the core (crust) region.

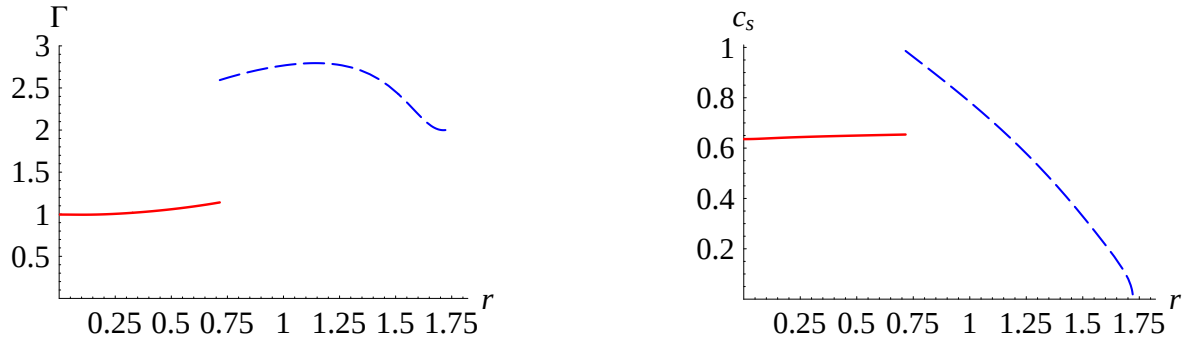

Figure 15: The adiabatic index at constant entropy (Γ) and the sound speed (c_s) distribution in the hypothetical multiquark star for the central density $\rho_0 = 20$ and $n_s = 0.3$. The inner (outer) red (dashed-blue) line represents the core (crust) region.

Figure 10 shows the pressure and density distribution within the multiquark star for the case of $n_s = 0$ for the central density $\rho_0 = 20$. Even though the density and pressure decrease rapidly with respect to the radius of the star, they never quite reach zero. It turns out that when the density and pressure reach the critical values where the equation of state changes into the different power-law for small d, the crust region continues for a large fraction of the total radius of the star. This makes the crust mass contribution to the total mass of the star dominant as is shown in Fig. 9.

Some remarks should be made regarding the hydrodynamic properties of the multiquark phase (taken as nuclear liquid). At constant temperature and entropy, we can define the adiabatic index

$$\Gamma \equiv \frac{\rho}{P}\frac{\partial P}{\partial \rho}, \tag{57}$$

$$= \frac{\rho}{P}c_s^2 \tag{58}$$

where c_s is the sound speed in the multiquark liquid. They depend on the equation of state of the multiquark and their distributions within the multiquark star are shown in Fig. 11 for $n_s = 0$. The sound speed never exceeds the speed of light in vacuum. It is also found that the adiabatic index and the sound speed change within a small fraction as the central densities are varied for a given n_s.

The multiquark star with $n_s = 0.3$ (having colour charges) converge to a smaller mass and radius at high central density (Fig. 12). Multiquarks with colour charges has lower pressure (and therefore smaller density) than the colourless ones for small density (Fig. 13). This smaller pressure makes the coloured multiquark star smaller and thus less massive than the colourless one. In more realistic situations, all of the possible multiquarks with varying n_s coexist in the multiquark phase. The mass limit and mass radius relation will vary between the two typical cases we consider here. Since the equations of state are found NOT to be sensitive to the temperature within the range between the gluon deconfinement and the chiral symmetry restoration, our results should also be valid even when the temperature varies within the star (but not too high and too low, of course).

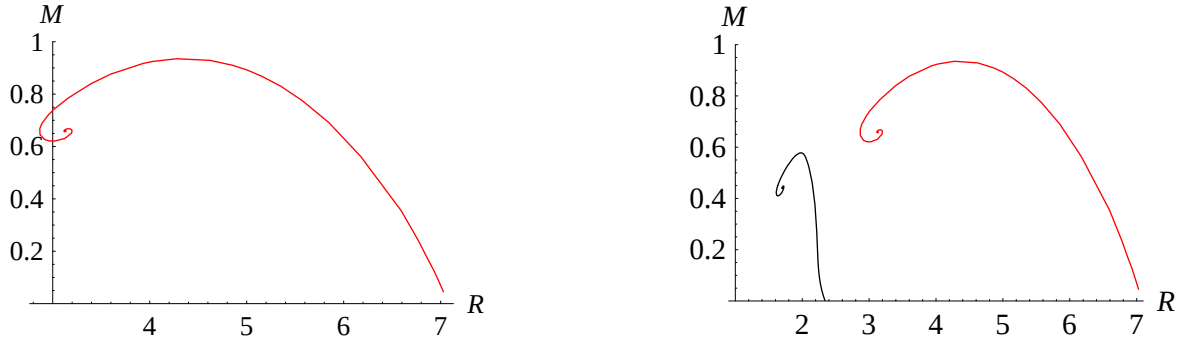

Figure 16: The relation between mass and radius of the multiquark star with (a) $n_s = 0$, (b) $n_s = 0$ (red) and $n_s = 0.3$ (black).

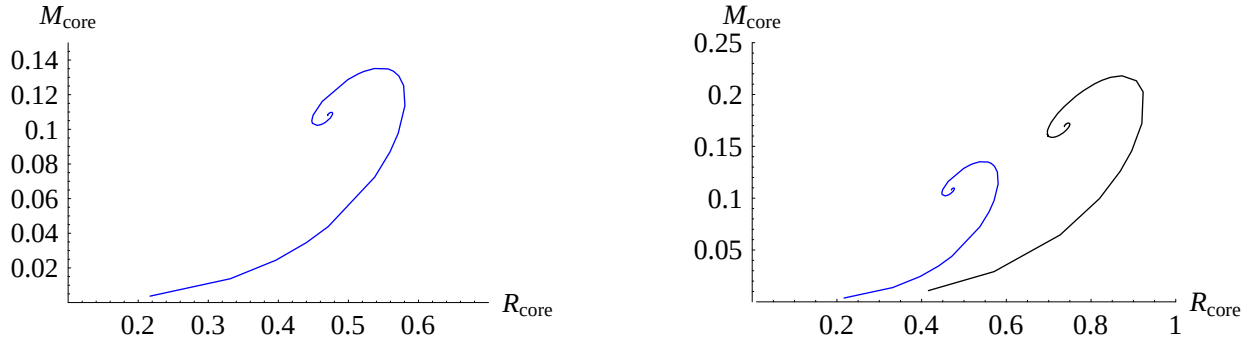

Figure 17: The relation between mass and radius of the core of the multiquark star with (a) $n_s = 0$, (b) $n_s = 0$ (blue) and $n_s = 0.3$ (black).

The baryon chemical potential distributions in the multiquark star for $n_s = 0, 0.3$ are shown in Fig. 14. In the core region, the chemical potential distributions of both cases are similar due to the similarity of the equations of state for large density. A small jump of the chemical potential at the transition radius between core and crust region is the artifact from the power-law approximation. The value of the chemical potential at the transition radius from the full expression which we used in the numerical simulations is slightly different from the approximated value using the power-law.

The adiabatic index and sound speed of the multiquark phase for $n_s = 0.3$ are shown in Fig. 15. The adiabatic index is higher than $n_s = 0$ case but the sound speed in the low density region is distinctively higher. Around the transition density, the sound speed reaches the maximum value of about 0.986 of the speed of light in vacuum. For both $n_s = 0, 0.3$ cases, it is obvious that the adiabatic index is closer to 1 in the core reflecting the fact that the density distribution is more condensed in the core region. The adiabatic index reaches $\lambda' = 2$ at the star surface since the the equation of state at zero density is $P \propto \rho^{\lambda'}$ (i.e. $\Gamma(\rho \to 0) = \lambda'$ for Eqn. (50)).

The *spiral* relation between mass and radius of the multiquark star is shown in Fig. 16. As the central density is increasing, the mass and radius of the $n_s = 0$ (0.3) multiquark star converge to the value of 0.659 (0.440) and 3.132 (1.704) respectively. For the core, the mass and radius of the core for $n_s = 0$ (0.3) converge to the value of 0.108 (0.169) and 0.471 (0.737).

Finally, we would like to estimate these limits of mass and radius in the physical units. Since our dimensionless quantities are related to the physical quantities through conversion factors given in Table 1 (Appendix A), both physical mass and radius vary with the energy density of the nuclear matter phase as $\propto 1/\sqrt{\text{energy density scale}}$. For a multiquark nuclear phase with energy density scale 10 GeV/fm^3, the conversion factor of the mass and radius are $5.91 M_{solar}$ and 8.71 km respectively. This would correspond to the converging mass and radius (in the limit of very large central density) of 3.89 (2.60)M_{solar} and 27.29 (14.85) km for $n_s = 0$ (0.3) multiquark star respectively.

In realistic situation, the nuclear phase in the outer region could lose heat out to the space in the form of radiation. The nuclear matter in the outer region of the crust will cool

down and mostly become confined into neutrons and hadrons (e.g. hyperons, pions). This would make the multiquark crust to end at shorter radius than the estimated value and render the multiquark star to be smaller and less massive than the estimated values in the hypothetical prototype. For example, for the energy density scale 10 GeV/fm^3, the critical density is $\rho_c \approx 1.5 \times 10^{18}$ kg/m^3 ($n_s = 0$). This is still a sufficiently large density for the neutron layer to be formed. If the temperature of the nuclear matter in the crust region falls below the deconfinement temperature, the multiquarks will be confined into extremely dense neutrons and hadrons instead. For a typical neutron star, the distance of the neutron layer out to the star surface is roughly 5-6 km [30]. If we add this number to the radius of the multiquark core, $0.471 \times 8.71 \simeq 4.10$ km, we end up with a more realistic estimation for the multiquark star with radius ~ 10 km. Regardless of the name, only the core region is in the deconfined multiquark phase and the content of the outer layers are the confined nucleons.

6 Discussions and conclusion

In the gluon-deconfined phase of the general Sakai-Sugimoto model, multiquark states can exist in the intermediate temperatures below the chiral symmetry restoration temperature provided that the density is sufficiently large. They are stable and preferred thermodynamically over other phases and thus they can play an important role in the physics of compact warm stars. By analytic and numerical methods, we demonstrate that the equation of state of the multiquark nuclear matter can be approximated by two power-laws in the small and large density region. Roughly speaking, the pressure is proportional to d^2 and $d^{7/5}$ for the small and large number density (d) regions respectively.

It is also found that the effect of the colour charges of the multiquark is to reduce the pressure of the multiquarks when the density is small. At higher densities, multiquarks with colour charges exert slightly larger pressure than the colourless ones. The temperature dependence of the entropy density shows an $s \propto T^5$ relation and the colour charge dependence $s_{colour} \propto n_s T$ (see Fig. 6 and Eqn. (39)). This implies that the multiquarks with colour charges have larger entropy but their number of degrees of freedom depend less sensitively on the temperature. Multiquarks in the deconfined phase behave like quasi-particles with the entropy density being less sensitive to the temperature than the gas of mostly free gluons and quarks in the χ_S-QGP phase.

Using the power-law equations of state for both small and large density regions, a spherically symmetric Einstein field equation is solved to obtain the Tolman-Oppenheimer-Volkoff equation. By solving this equation numerically, we establish the mass, density and pressure distribution of the hypothetical multiquark star. It turns out that the multiquark star is separated into two layers, a core with higher density and a crust with lower density. Mass limit curve is also obtained as well as the mass sequence plot between the mass and radius of the multiquark star. They show typical spiral behaviour of the star sequence plots. The mass limit curve shows two peaks corresponding to the equation of state of the small and the large density. Analyses show that the most contribution to the total mass is mainly

from the crust. The adiabatic index at constant entropy, Γ, and the sound speed, c_s, of the multiquark nuclear phase within the star are calculated numerically. For large density, Γ is approximately close to 1 and c_s is roughly within range $0.6 - 0.7$ of the speed of light. For small density, Γ is in the range $1.3 - 2.0$ $(2.0 - 3.0)$ and c_s is roughly $0 - 0.85$ $(0 - 0.99)$ for multiquark with $n_s = 0$ (0.3).

Acknowledgments

P.B. is supported in part by the Thailand Research Fund (TRF) and the Commission on Higher Education (CHE) under grant MRG5180227. E.H. is supported by the Commission on Higher Education (CHE), Thailand under the program Strategic Scholarships for Frontier Research Network for the Ph.D. Program Thai Doctoral Degree for this research.

A Dimensional translation table

quantity	dimensionless variable	physical variable
pressure	P	$\frac{c^4}{Gr_0^2}P$
density	ρ	$\frac{c^2}{Gr_0^2}\rho$
mass	M	$\frac{r_0c^2}{G}M$
radius	r	$r_0 r$

Table 1: Dimensional translation table of relevant physical quantities, $r_0 \equiv \left(\frac{G\mathcal{N}}{c^4\tau V_3}\right)^{-1/2} = \left(\frac{G}{c^4}(\text{energy density scale})\right)^{-1/2}$.

References

[1] F. Karsch, "Lattice QCD at finite temperature," AIP Conf. Proc. **631** (2003) 112.

[2] Marco Panero, "Thermodynamics of the QCD plasma and the large-N limit," *Phys. Rev. Lett.* **103** (2009) 232001, [arXiv:0907.3719].

[3] E. V. Shuryak, I. Zahed, "Towards a theory of binary bound states in the quark gluon plasma," *Phys. Rev.* **D70** (2004) 054507, [arXiv:hep-ph/0403127].

[4] E. V. Shuryak, I. Zahed, "Rethinking the properties of the quark gluon plasma at $T \sim T_c$", *Phys. Rev.* **C70** (2004) 021901, [arXiv:hep-ph/0307267].

[5] J. Liao, E.V. Shuryak, "Polymer chains and baryons in a strongly coupled quark-gluon plasma,"*Nuc. Phys.* **A775** (2006) 224, [arXiv:hep-th/0508035].

[6] J. M. Maldacena, "The Large N Limit of Superconformal Field Theories and Supergravity," *Adv. Theor. Math. Phys.* **2** (1998) 231-252 [*Int. J. Theor. Phys.* **38** (1998) 1113-1133], [arXiv:hep-th/9711200].

[7] Juan M. Maldacena, "Wilson loops in large N field theories," *Phys. Rev. Lett.* **80** (1998) 4859-4862, [arXiv:hep-th/9803002].

[8] Soo-Jong Rey, Jung-Tay Yee, "Macroscopic strings as heavy quarks in large N gauge theory and anti-de Sitter supergravity," *Eur. Phys. J.* **C 22** (2001) 379-394, [arXiv:hep-th/9803001].

[9] Soo-Jong Rey, Stefan Theisen, Jung-Tay Yee, "Wilson-Polyakov loop at finite temperature in large N gauge theory and anti-de Sitter supergravity," *Nucl. Phys.* **B 527** (1998) 171-186, [arXiv:hep-th/9803135].

[10] E. Witten, "Baryons and Branes in Anti-de Sitter Space," *JHEP* **07** (1998) 006, [arXiv:hep-th/9805112].

[11] D. J. Gross and H. Ooguri, "Aspects of large N gauge theory dynamics as seen by string theory," *Phys. Rev.* **D58** (1998) 106002, [arXiv:hep-th/9805129].

[12] A. Brandhuber, N. Itzhaki, J. Sonnenschein and S. Yankielowicz, "Baryon from supergravity," *JHEP* **07** (1998) 046, [arXiv:hep-th/9806158].

[13] K. Ghoroku, M. Ishihara, A. Nakamura and F. Toyoda, "Multi-Quark Baryons and Color Screening at Finite Temperature," *Phys. Rev.* **D79** (2009) 066009, [arXiv:0806.0195 [hep-th]].

[14] K. Ghoroku and M. Ishihara, "Baryons with D5 Brane Vertex and k-Quarks States," *Phys. Rev.* **D77** (2008) 086003, [arXiv:0801.4216 [hep-th]].

[15] M.V. Carlucci, F. Giannuzzi, G. Nardulli, M. Pellicoro and S. Stramaglia, "AdS-QCD quark-antiquark potential, meson spectrum and tetraquarks," *Eur. Phys. J.* **C57** (2008) 569, [arXiv:0711.2014 [hep-ph]].

[16] W-Y. Wen, "Multi-quark potential from AdS/QCD," *Int. J. Mod. Phys.* **A23** (2008) 4533, [arXiv:0708.2123 [hep-th]].

[17] P. Burikham, A. Chatrabhuti and E. Hirunsirisawat, "Exotic multi-quark states in the deconfined phase from gravity dual models," *JHEP* **05** (2009) 006, [arXiv:0811.0243 [hep-ph]].

[18] T. Sakai and S. Sugimoto, "Low Energy Hadron Physics in Holographic QCD," *Prog. Theor. Phys.* **113** (2005) 843, [arXiv:hep-th/0412141].

[19] T. Sakai and S. Sugimoto, "More on a Holographic Dual of QCD," *Prog. Theor. Phys.* **114** (2005) 1083, [arXiv:hep-th/0507073].

[20] O. Aharony, J. Sonnenschein and S. Yankielowicz, "A Holographic Model of Deconfinement and Chiral Symmetry Restoration," *Annals Phys.* **322** (2007) 1420, [arXiv:hep-th/0604161].

[21] J.R. Oppenheimer and G.M. Volkoff, "On Massive Neutron Cores," *Phys. Rev.* **55** (1939) 374, R.C. Tolman, "Static solutions of Einstein's field equations for spheres of fluid," *Phys. Rev.* **55** (1939) 364.

[22] Oren Bergman, Gilad Lifschytz, Matthew Lippert, "Holographic Nuclear Physics," *JHEP* **11** (2007) 056, [arXiv:hep-th/0708.0326].

[23] C. G. Callan, A. Guijosa and K. G. Savvidy, "Baryons and String Creation from the Fivebrane Worldvolume Action," *Nucl. Phys.* B 547 (1999) 127 [arXiv:hep-th/9810092].

[24] C. G. Callan, A. Guijosa, K. G. Savvidy and O. Tafjord, "Baryons and Flux Tubes in Confining Gauge Theories from Brane Actions," *Nucl. Phys.* B 555 (1999) 183 [arXiv:hep-th/9902197].

[25] N. Horigome and Y. Tanii, "Holographic chiral phase transition with chemical potential," *JHEP* **01** (2007) 072, [arXiv:hep-th/0608198].

[26] K. Y. Kim, S. J. Sin and I. Zahed, "Dense hadronic matter in holographic QCD," [arXiv:hep-th/0608046].

[27] A. Akmal, V.R. Pandharipande, and D.G. Ravenhall, "The equation of state of nucleon matter and neutron star structure", *Phys. Rev.* **C58** (1998) 1804, [arXiv:nucl-th/9804027].

[28] Keun-Young Kim, Sang-Jin Sin, Ismail Zahed, "The Chiral Model of Sakai-Sugimoto at Finite Baryon Density", *JHEP* **01** (2008) 002, [arXiv:0708.1469 [hep-th]].

[29] J. de Boer, K. Papadodimas and E. Verlinde, "Holographic Neutron Stars," [arXiv:0907.2695 [hep-th]].

[30] F. Weber, "Strange Quark Matter and Compact Stars", *Prog. Part. Nucl. Phys.* **54** (2005) 193, [arXiv:astro-ph/0407155].